A Database of CFD-based Buffet Forcing Functions for Artemis I Structural Response Evaluation

Francesco Soranna, Craig L. Streett, Patrick Heaney, Martin Sekula, David Piatak, Oleg Goushcha, and Michael Ramey
NASA Langley Research Center, Aeroelasticity Branch

Acknowledgments: SLS Aerodynamics across NASA

AIAA SciTech Forum, January 6-10, 2025

Photo Source: NASA

Outline

1. **Introduction.**
2. **Objective of the present work.**
3. **CFD time accurate simulations.**
4. **Comparison of unsteady pressures: flight vs. simulation.**
5. **Buffet forcing functions database.**
6. **Conclusions.**

Artemis I flight test vehicle on Launch Complex 39B (November 2022). [Source: NASA]

Introduction

- **During ascent, transonic buffet is a major source of structural excitation on the Space Launch System.**
  - In the design of a launch vehicle, buffet-induced unsteady forces must be well characterized and accounted for.

- **Databases of buffet-induced unsteady forces are typically based on wind-tunnel data. Wind-tunnel data present certain limitations:**
  - Freestream Mach number < ~1.2.
  - Reynolds number is one order of magnitude smaller than the flight Reynolds number.
  - Stationary flow conditions (no wind-tunnel can produce flight-equivalent flow accelerations).
  - Discrete pressure measurements.

- **Flight tests help remove some of the above-mentioned limitations but present other challenges such as cost, limited sensors density, sensor loss. Furthermore, flight data contain nonbuffet related excitations (e.g., gusts, acoustics) that can be challenging to separate out.**

- **Advanced CFD provides a viable means to fill some of the gaps existing in the experiments and to separate the impact of different excitation contributors.**

Objective of This Work

1. **To establish a level of confidence in the ability of CFD to estimate buffet-related environments under accelerating-flow conditions (as experienced by the SLS during Artemis I).**

2. **To utilize these CFD data to develop a database of buffet unsteady forces that includes the effects of accelerating-flow conditions.**

   – Of particular interest is to address how well buffet forces obtained from accelerating-flow simulations compare to their counterpart based on wind-tunnel-like conditions (i.e., stationary flow conditions).

CFD Time Accurate Simulations

- **The CFD simulations were conducted using NASA's FUN3D code. These simulations utilized the improved delayed detached-eddy (iDDES) turbulence model, with the Spalart-Allmaras (SA-neg) RANS model.**
- **Time-accurate mesh translations were also utilized to simulate the changing velocity and attitude based on the Artemis I best estimated trajectory (BET).**
- **The simulations utilized the Block 1 Cargo forebody, rather than the Block 1 Crew that was flown during Artemis I.**

CFD mesh

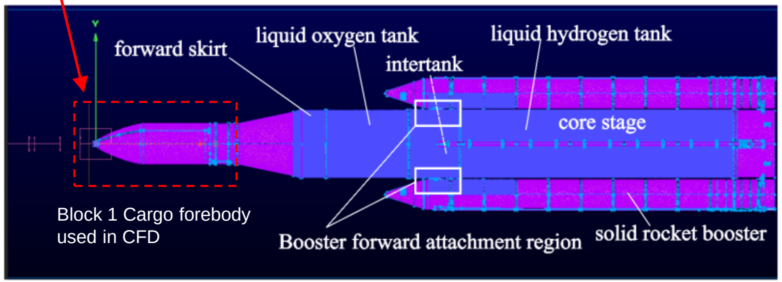

Block 1 Crew forebody flown during Artemis I

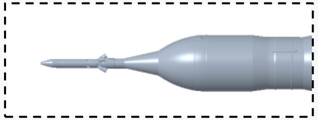

- **Two sets of FUN3D simulations were conducted:**
  - **- Set# 1: Accelerating-flow simulations:** $M_\infty \in [0.8\ ,1.92]$ **(flight-like simulations)**
  - **- Set# 2: Constant** M_∞ **simulations:** $M_\infty \in \{0.95,1.18,1.70\}$ **(wind-tunnel-like simulations)**

Flight vs. Simulation
Unsteady Pressures

Flight vs. Accelerating-Flow Simulation: C_p'

- During the Artemis I flight, pressure data from 183 pressure transducers were acquired throughout ascent to observe the external pressure environments and to compare with preflight predictions based on wind-tunnel testing.
- The accelerating-flow FUN3D surface pressures were compared to those measured by pressure transducers installed on the Artemis I flight test vehicle.
- Below is a comparison of bandpass filtered C_p' versus M_∞ for an Artemis I flight sensor at a sample analysis location and the nearest neighbor CFD node.
- Trends of peak-to-peak C_p' magnitude of flight vs. simulation are in good agreement.

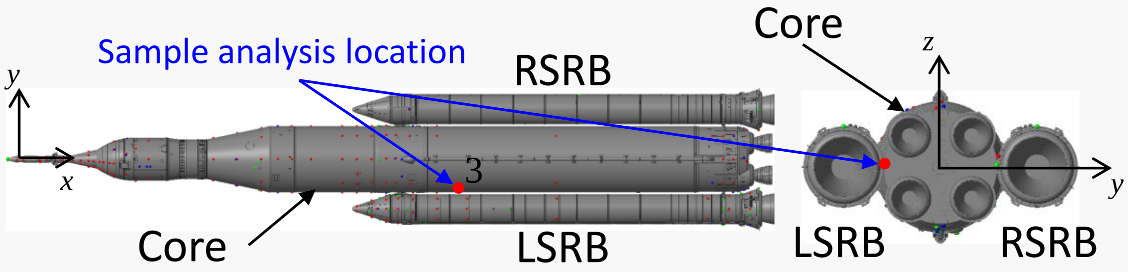

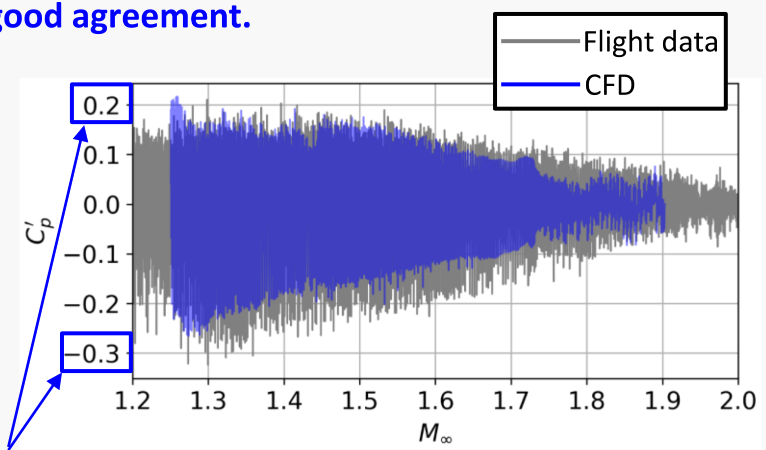

Note: very large peak-to-peak C_p' magnitude

Flight vs. Accelerating-Flow Simulation: $C'_{p,rms}$

- **On the right: comparison of band-pass filtered $C'_{p,rms}$ versus M_∞ for Artemis I flight sensors at sample analysis locations and the corresponding nearest neighbor CFD nodes.**

Reasonable agreement between flight and CFD data

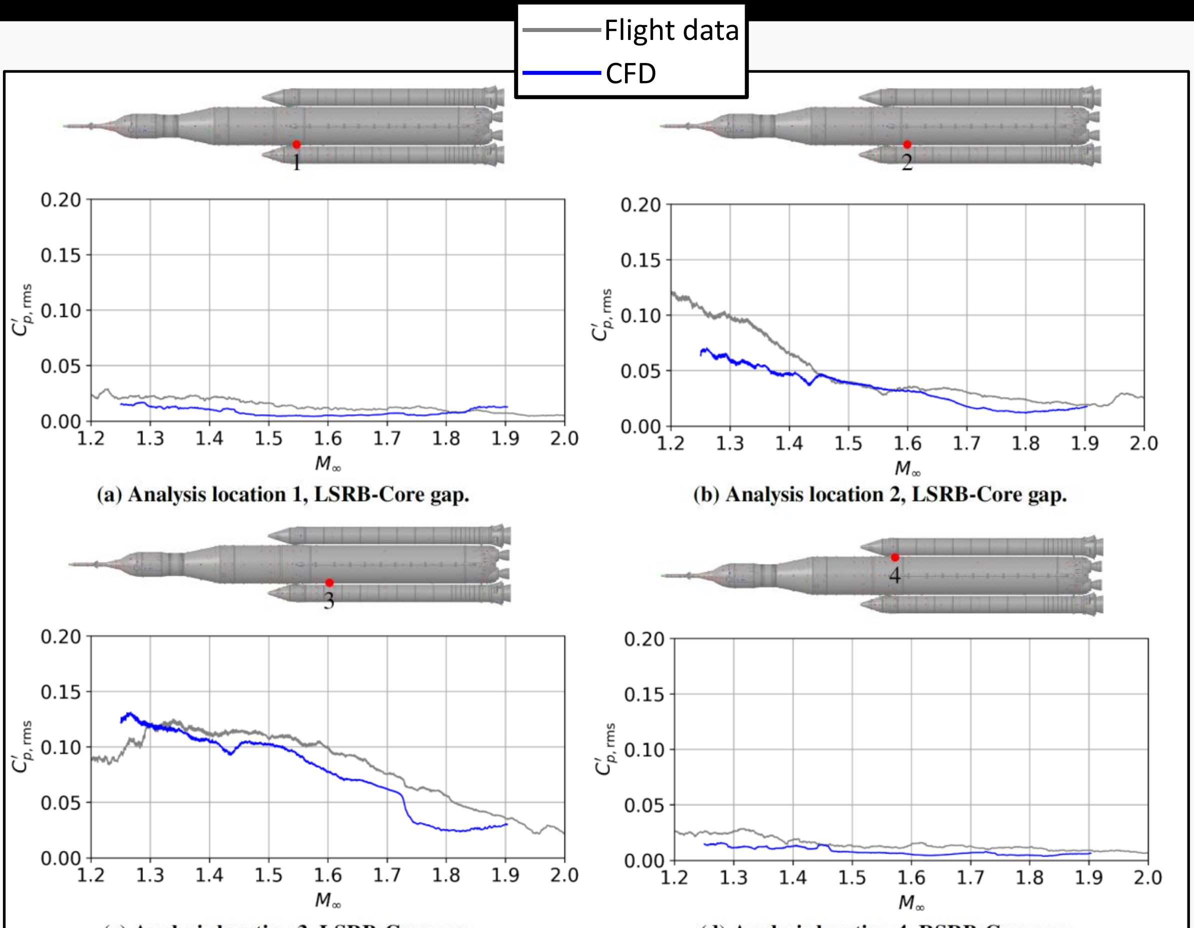

(a) Analysis location 1, LSRB-Core gap.
(b) Analysis location 2, LSRB-Core gap.
(c) Analysis location 3, LSRB-Core gap.
(d) Analysis location 4, RSRB-Core gap.

Spectrograms of C_p' vs. (M_∞, frequency)

- **Artemis I and CFD spectrograms demonstrate broadly similar features, in particular:**
  (A) relatively constant frequency peaks corresponding to pressure modes in the lower supersonic flight ($M_\infty \in [1.25, 1.70]$) and **(B)** rapid increase in these frequency peaks at approximately $M_\infty = 1.70$.

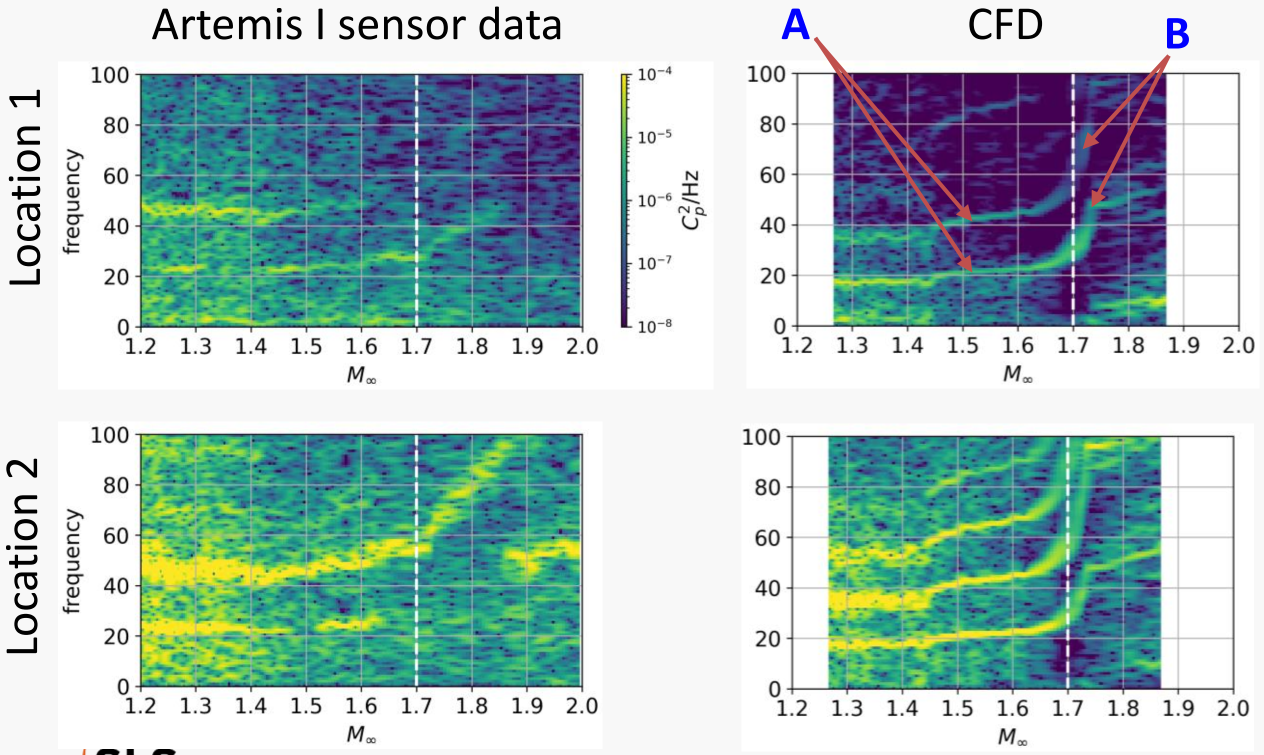

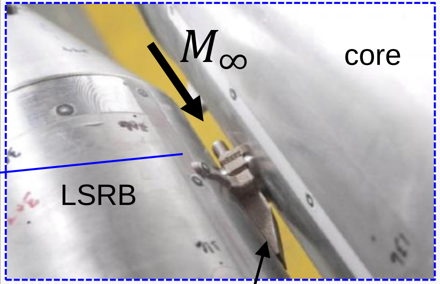

- A wake is produced by the forward attachment hardware between the core stage and SRBs.
- Shedding within this wake is responsible for the frequency peaks shown in **(A)** and **(B).**

Buffet Unsteady Forces

CFD-Based Buffet Forcing Functions Database Development

- Let F_i define the unsteady component of a point force acting along the i-axis on the centerline of the core stage or on the boosters' centerline.
- An unsteady sectional force is defined as $f_i(x,t) = \partial F_i/\partial x\ (i = y, z)$, where t is time and dx is an arbitrarily small spacing between longitudinal planes on the core or on the solid rocket booster. From now on, both F_i and f_i are referred to as **Buffet Forcing Functions (BFFs)**, either point BFFs (F_i) or sectional BFFs (f_i).
- Focusing on the core stage, f_i were calculated at 261 longitudinal locations based on direct integration of the CFD unsteady pressures. The spacing dx between these 261 longitudinal locations is $dx/D = 0.025$ where D is the reference core stage diameter.
- The next slides shows comparisons of root-mean-square trends of the unsteady forces based on accelerating-flow simulations and stationary flow simulations.

f_y : centerline unsteady force/length (sectional BFF) acting along y on a sample longitudinal location on the core stage

Vertical lines: sample longitudinal locations where the BFFs are calculated

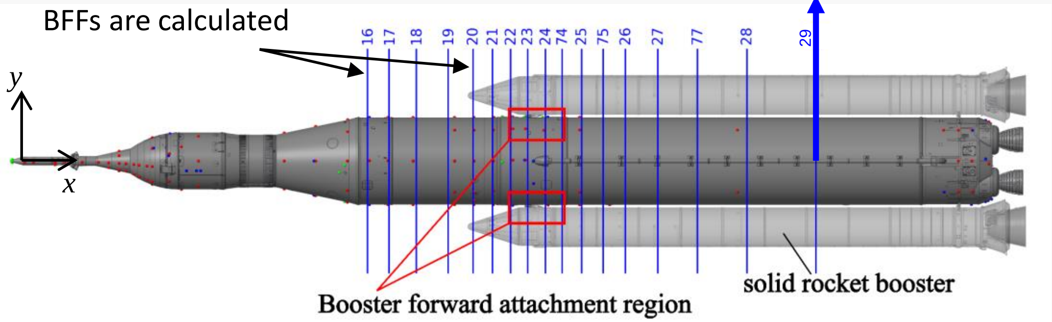

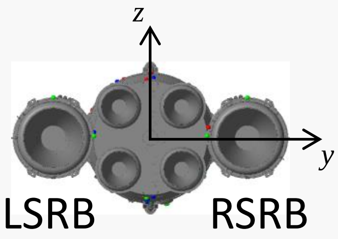

Distribution of Unsteady Forces $f_{yz,rms}$, $M_\infty = 0.95$

Plot below: rms distribution of band-passed filtered $f_{y,rms}$ and $f_{z,rms}$ unsteady forces on the core stage based on accelerating-flow simulation data (in blue) and constant M_∞ simulation data (in red).

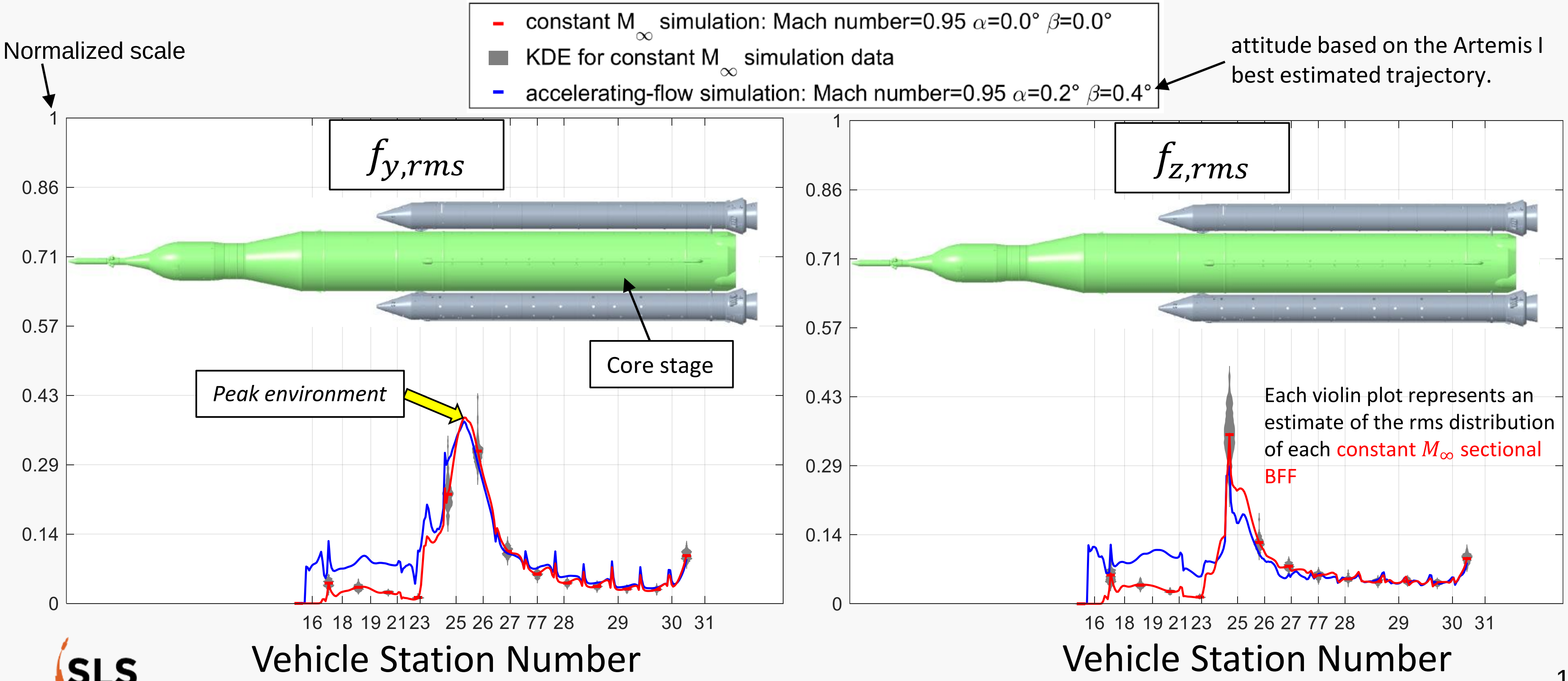

Distribution of Unsteady Forces $f_{yz,rms}$, $M_\infty = 1.18$

Overall, there is a good agreement between $f_{yz,rms}$ levels based on accelerating-flow simulation and constant M_∞ simulation data for the Mach numbers presented in the paper.

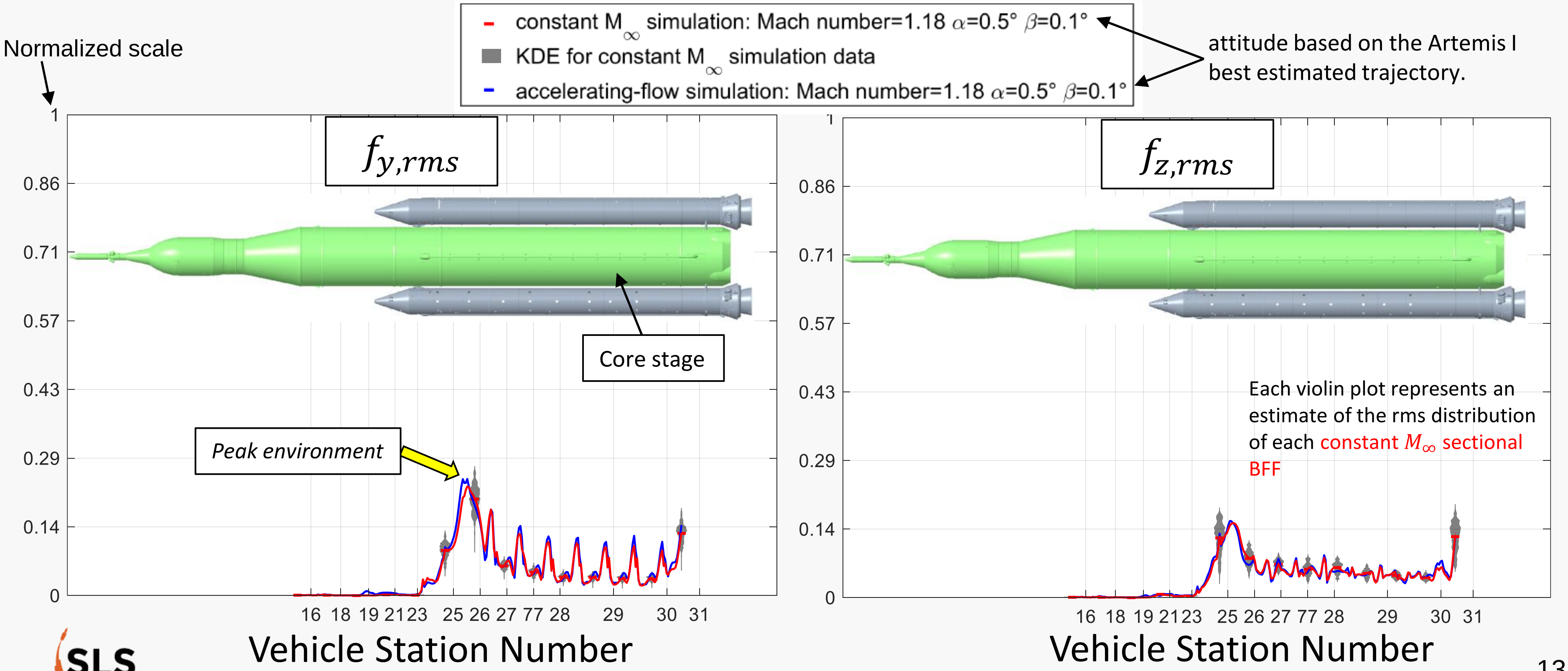

Power Spectral Density of f_i , $M_\infty = 1.18$

Plots on the right: PSD trends of unsteady forces f_y and f_z based on accelerating-flow simulation (in blue) and constant M_∞ simulation (in red) at a sample station near the peak buffet environment. Attitude closest to flight α, β.

Observations:

- Both accelerating-flow and constant M_∞ data contain peaks associated with shedding off the booster forward attachment.
- After accounting for dispersion (gray patch), the accelerating-flow PSD of the unsteady forces are mostly enveloped by the constant M_∞ PSDs.

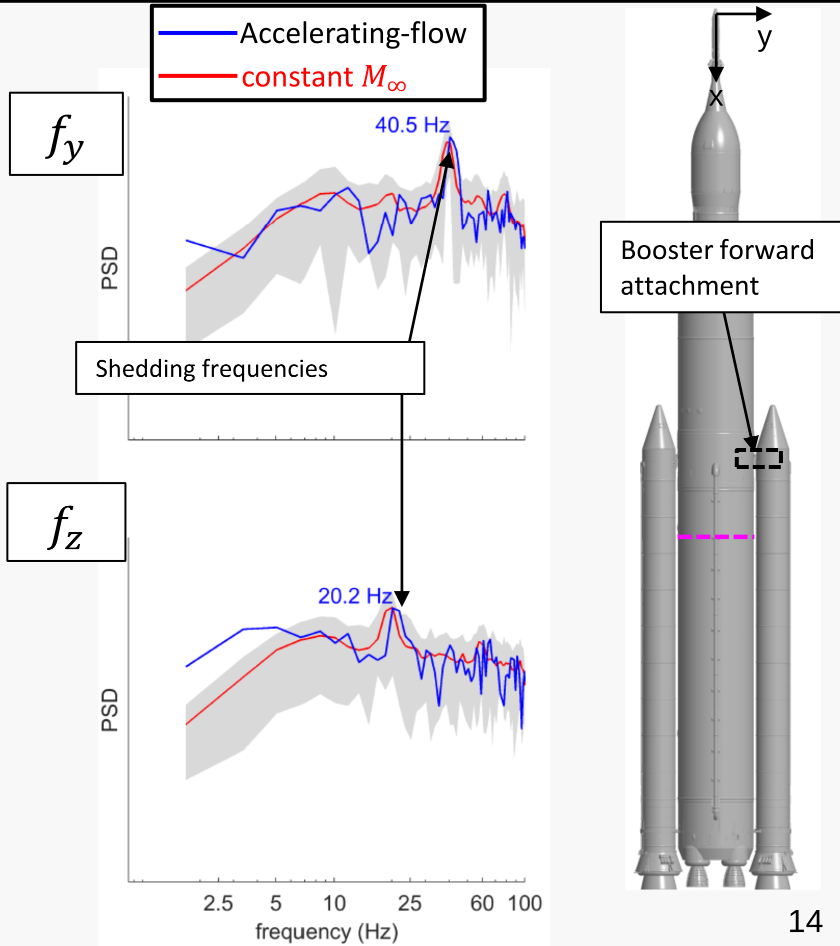

Conclusions

- **Accelerating-flow CFD provides a satisfactory estimation of the Artemis I peak buffet environment.**
- **For this vehicle and trajectory, BFFs that are derived from flight-like simulations, which include the effects of vehicle acceleration, are well represented by BFFs based on wind-tunnel-like simulations that assume stationary flow conditions.**
- **Future work could investigate how the pressure field spatial resolution impacts the present accelerating-flow BFF database.**

Thank you!